ACAVIS PUBLISHERS

Journal of Surgery and Operative Techniques

Research Article

Volume 1, Issue 1

Profiles Binocular Wavefront Imbalance in Myopic Anisometropia: Corneal Surface Asymmetry as the Dominant Optical Determinant

Guan X , Kang M , Zhang L , Fu C , Dong Y , Ma D , Zhai C , Zheng Y*

Beijing Tongren Eye Center, Beijing Key Laboratory of Ophthalmology and Visual Science, Beijing Tongren Hospital, Capital Medical University, China

***Correspondence:**
Yan Zheng
No. 1 Dong Jiao Min Xiang Street, Dongcheng District, Beijing, China.
Email: trzhengyan@163.com

Article Info:
Received Date: June 14, 2026
Published Date: June 30, 2026

Citation:
Guan X, Kang M, Zhang L, Fu C, Dong Y, Ma D, Zhai C, Zheng Y. Binocular Wavefront Imbalance in Myopic Anisometropia: Corneal Surface Asymmetry as the Dominant Optical Determinant. J Surg Operative Tech. 2026;1(1):1-12.

ABSTRACT

Purpose: To characterize higher-order aberration (HOA) profiles and their interocular asymmetry in myopic anisometropia, and to identify the structural corneal determinants of binocular optical imbalance.

Methods: In this retrospective cross-sectional study, 71 adults with myopic anisometropia (interocular spherical equivalent difference ≥2.00 D) and 71 isometropic controls were evaluated using the OPD-Scan III integrated platform. Wavefront data were decomposed via Zernike polynomials over a 6.0-mm pupil to extract total ocular, corneal, and internal HOAs. Interocular HOA asymmetry was quantified as absolute interocular differences. Group comparisons employed Kruskal-Wallis and Mann-Whitney U tests; generalized estimating equation (GEE) models assessed independent associations with anisometropia. Spearman correlation and multivariable linear regression identified predictors of interocular HOA asymmetry.

Results: At the single-eye level, GEE analysis revealed that corneal trefoil was the sole HOA parameter independently elevated in anisometropic eyes (β = 0.0510; 95% CI: 0.0186–0.0833; P = .002), scaling continuously with anisometropia severity. Despite comparable absolute HOA magnitudes between groups, anisometropic participants demonstrated significantly greater interocular asymmetry in total ocular, corneal, and internal HOAs, with corneal coma asymmetry showing the most pronounced between-group difference (median |Δ|: 0.082 vs. 0.054 μm; P = .004; Cohen's d = 0.544). Neither interocular spherical equivalent difference nor absolute refractive error correlated with HOA asymmetry. The absolute interocular difference in the surface asymmetry index (|ΔSAI|) emerged as the dominant independent predictor of corneal coma asymmetry (β = 0.589; P < .001), total corneal HOA asymmetry (β = 0.423; P = .002), and internal HOA asymmetry (β = 0.682; P = .007).

Conclusion: The optical consequences of myopic anisometropia are better characterized as binocular wavefront imbalance than as unilateral aberrational excess. Corneal trefoil specifically tracks anisometropia severity, while interocular HOA asymmetry

is governed primarily by corneal surface irregularity asymmetry rather than refractive disparity. Comprehensive optical evaluation of anisometropic patients should incorporate binocular wavefront compatibility and corneal topographic symmetry indices beyond spherical equivalent differences alone.

KEYWORDS: Myopic anisometropia, Higher-order aberrations, Interocular asymmetry, Corneal wavefront, Binocular optical imbalance, OPD-Scan III

INTRODUCTION

Anisometropia, commonly defined as an interocular spherical equivalent difference of ≥1.00 diopter (D), is reported in approximately 1%–11% of population- and schoolbased samples[1-3], with prevalence decreasing markedly (to roughly 1%–3%) as the diagnostic threshold increases to ≥2.00 D[4,5].Clinically, this refractive mismatch induces inconsistent retinal image states between the two eyes, thereby compromising overall binocular image quality[6,7]. During visual development, this optical disparity drives the brain to competitively suppress the more defocused eye, leading to the onset of amblyopia and persistently impairing stereoacuity, binocular contrast sensitivity, and fusional vergence[8-10] . Fundamentally, these refractive and subsequent neural deficits are rooted in asymmetric anatomical development of the ocular refractive media, characterized by interocular variations in corneal shape, lens thickness, or axial elongation[11,12]. These structural asymmetries may translate into interocular differences in higher-order aberrations (HOAs) at the wavefront level, further degrading binocular optical quality beyond mere low-order defocus[13,14]. Therefore, elucidating the optical underpinnings of anisometropia, specifically the interocular HOA asymmetry, is critical not only for a comprehensive understanding of developmental visual science but also for optimizing clinical decision-making in modern refractive surgery.

Wavefront aberrometry provides a quantitative characterization of optical quality that extends beyond conventional low-order refractive errors. However, comprehensively assessing the wavefront profile of anisometropic eyes requires an integrated optical approach. Traditional standalone corneal topographers lack total and internal ocular data, rendering them insufficient for uncovering internal optical discrepancies.[15] Meanwhile, conventional Hartmann-Shack aberrometers often face constraints in highly aberrated eyes due to limited sampling points.[16,17] To overcome these diagnostic limitations, modern integrated platforms, such as the OPD-Scan III, utilize dynamic spatial skiascopy combined with Placido-disk technology. Utilizing this integrated diagnostic approach uniquely enables the precise optical attribution of interocular differences across various refracting interfaces, thereby addressing the incompletely resolved contributions of corneal and lenticular factors.

Previous work has largely characterized the optics of ametropia using singleeye wavefront analysis, comparing ocular or corneal higherorder aberrations (HOAs) across refractive error groups such as myopic, hyperopic and emmetropic eyes. Several studies have reported higher levels of total HOAs and specific terms such as spherical aberration and coma in eyes with greater refractive error, including high myopia, compared with emmetropic eyes[18,19]. These elevations have been linked to axial elongation and associated changes in anterior segment geometry, including corneal shape and crystalline lens morphology[19,20]. However, important limitations remain. First, most existing work compares HOA magnitudes across refractive groups using one eye per subject, without explicitly quantifying interocular HOA asymmetry, defined as the withinsubject mismatch in wavefront profile between the two eyes, which is arguably most relevant to binocular visual function. Second, prior studies have seldom disentangled the relative contributions of corneal topographic irregularity versus the magnitude of interocular refractive disparity to binocular optical imbalance. Third, the association between anisometropia magnitude and specific HOA subtypes has received little direct investigation. As a result, the structural corneal and optical determinants of binocular wavefront asymmetry in anisometropia remain poorly defined.

To address these gaps, a retrospective cross-sectional study was conducted using the OPD-Scan III platform to comprehensively evaluate the optical characteristics of myopic anisometropia. Specifically, the present study aimed to: (1) compare HOA profiles and their interocular asymmetry between patients with myopic anisometropia and isometropic controls; (2) explore the independent association between the anisometropic condition and absolute HOA magnitudes; and (3) identify the clinical predictors of interocular HOA asymmetry through correlation and multivariable regression analyses.

METHODS

Study Design and Participants

This retrospective, cross-sectional study enrolled consecutive patients who underwent comprehensive optical quality assessment using the OPD-Scan III system (NIDEK Co., Ltd., Gamagori, Japan) at the Refractive Surgery Center of Beijing Tongren Hospital between January 2025 and July 2025. Eligible participants were adults aged 18 to 40 years.

Subjects were classified into two groups based on the magnitude of interocular refractive difference. The anisometropic group comprised individuals with an interocular difference in spherical equivalent (SE) ≥ 2.00 diopters (D). The isometropic (control) group comprised eyes with an interocular SE difference < 1.00 D and an interocular cylindrical difference < 1.00 D. To ensure distinct phenotypic separation between the two cohorts, patients with an interocular SE difference between 1.00 and 1.99 D were excluded. Within each group, eyes were further designated as the eye with the greater (Aniso Higher or Iso Higher) or lesser (Aniso Lower or Iso Lower) magnitude of myopia.

Exclusion criteria encompassed any history or clinical evidence of corneal disease (including keratoconus or forme fruste keratoconus), prior ocular surgery, active ocular inflammation, glaucoma, retinal disease, clinically significant dry eye, or any condition that could compromise optical quality measurements.

The study adhered to the tenets of the Declaration of Helsinki. The study protocol was approved by the Institutional Review Board of Beijing Tongren Hospital. Written informed consent for the

clinical examinations and the subsequent use of clinical data for research was obtained from all participants.

OPD-Scan III Measurement System

All measurements were obtained using the OPD-Scan III (NIDEK Co., Ltd., Gamagori, Japan), an integrated diagnostic platform combining wavefront aberrometry, Placido-disk corneal topography, and automated refractometry.

Prior to measurement, participants underwent dark adaptation in a fully darkened examination room for 10 minutes to facilitate natural pupillary dilation and relax accommodation. To capture both photopic and mesopic parameters, the device's automated internal light source was utilized to modulate the illumination conditions.

To optimize tear film stability and corneal coverage, a standardized acquisition protocol was employed. Participants were instructed to perform several complete blinks immediately before measurement; image acquisition commenced within 2 seconds of the final blink, ensuring optimal post-blink optical quality. The device automatically acquired a minimum of three consecutive scans. If reproducibility met the manufacturer's quality criteria, the session was accepted. The final output represented the average of accepted measurements with the highest quality indices.

Aberrometry Principles and Parameter Extraction

The OPD-Scan III evaluates total ocular aberrations based on dynamic spatial skiascopy. Specifically, a slit of infrared light is projected into the eye and rotated at 1° increments over a full 360°. This mechanism captures 2,520 data points, enabling the precise plotting of wavefront aberrations for pupil diameters up to 9.50 mm[21]. Concurrently, a Placido-disk system projects concentric rings onto the anterior corneal surface to independently derive corneal topography and corneal wavefront aberrations.

For the present analysis, wavefront data were decomposed using Zernike polynomials over a standardized 6.0-mm pupil diameter to yield quantitative metrics for total ocular, corneal, and internal aberrations. Internal aberrations were calculated via vector subtraction of the corneal from the total ocular components. The extracted aberration parameters comprised the root mean square (RMS) amplitudes of spherical aberration, coma, and trefoil, in addition to total higher-order aberrations (HOAs; defined as the RMS of the 3rd- through 6th-order Zernike terms). Furthermore, the analysis included steep and flat simulated keratometry (SimK), corneal asphericity (Q-value evaluated over a 6.0-mm diameter), and specific corneal regularity indices: the surface regularity index (SRI) and surface asymmetry index (SAI).

Outcome Measures

Primary outcomes encompassed: (1) interocular higher-order aberration asymmetry at the ocular, corneal, and internal levels, expressed as the absolute interocular difference ($|\Delta|$) in each HOA parameter, and (2) within-group paired comparisons of HOA values between the higher- and lower-refraction eyes.

Secondary analyses examined the association between HOA magnitude and anisometropia degree using generalized estimating equation (GEE) models, and explored the relationships between corneal morphological parameters and interocular HOA asymmetry using correlation and multivariable regression analyses.

Statistical Analysis

All statistical analyses were performed using R (version 2024.12.1). Data normality was evaluated via the Shapiro-Wilk test, with descriptive statistics presented as mean ±standard deviation or median [interquartile range] accordingly. Baseline characteristics were compared using the Mann-Whitney U or chi-square test. Cross-group comparisons among the four eye subgroups were conducted using the Kruskal-Wallis test, followed by Bonferroni-corrected post-hoc Mann-Whitney U tests.

To account for the paired-eye structure within participants (interocular correlation), generalized estimating equation (GEE) models with an exchangeable working correlation structure were employed. In these models, the absolute HOA value of each eye was inputted as the dependent variable, and group (anisometropia vs. isometropia) was specified as the primary independent variable, adjusting for potential confounding factors including spherical equivalent, age, and sex.

Within-group paired HOA comparisons utilized the Wilcoxon signed-rank test. Between-group differences in absolute interocular HOA asymmetry ($|\Delta|$ HOA) were evaluated with the Mann-Whitney U test, computing Cohen's d for effect size. Spearman correlation and multivariable linear regression (inclusion threshold: $P < .10$) were used to identify independent predictors of $|\Delta|$ HOA. Multicollinearity among independent variables in the regression models was assessed using the variance inflation factor (VIF). The Benjamini-Hochberg false discovery rate (FDR) correction was applied for multiple comparisons. A post-hoc power analysis was conducted to assess the adequacy of the sample size. With $n = 71$ per group and a two-sided α of 0.05, the study achieved >89% power to detect the observed between-group differences in corneal HOA parameters (Cohen's $d = 0.54–0.56$), and >94% power to detect the strongest Spearman correlations identified ($|rs| = 0.40–0.41$). For medium effect sizes (Cohen's $d = 0.47$; $|rs| = 0.33$), 80% power was achievable at the given sample size. Comparisons involving smaller effect sizes ($d < 0.42$; $|rs| < 0.30$) were associated with power below 70%, and negative findings in these analyses should therefore be interpreted as insufficient evidence to exclude a true association, rather than evidence of absence. All tests were two-sided, with $P < .05$ considered statistically significant.

RESULTS

Participant and Ocular Characteristics

The anisometropic ($n = 71$) and isometropic ($n = 71$) groups were matched in age ($P = .153$) and sex distribution ($P = .107$) (Table 1). Eyes were assigned to four subgroups based on the magnitude of refractive error: Aniso Higher, Aniso Lower, Iso Higher, and Iso Lower. Spherical equivalent and sphere varied significantly across these four subgroups (both $P < .001$). Post-hoc analysis showed that the Aniso Lower eye had a significantly lower magnitude of myopia than the other three subgroups. In contrast, the Aniso Higher eye

showed no statistically significant difference in spherical equivalent from either isometropic subgroup.

No significant differences were observed across the four subgroups in keratometric and morphologic parameters, including steep and flat keratometry, Q-value, surface regularity index (SRI), and surface asymmetry index (SAI) (all P > .05). Additionally, angle kappa showed no significant variation under either photopic (P = .812) or mesopic (P = .322) conditions.

Table 1. Breakdown of errors by number and percent of cases.

Characteristic	Anisometropia (n = 71)		Isometropia (n = 71)		P Value
Age, years	23.00 [19.00–29.00]		24.00 [20.00–31.50]		0.153
Sex, n (%)					0.107
Male	28 (39.4%)		18 (25.4%)		
Female	43 (60.6%)		53 (74.6%)		
Characteristic	Aniso Higher	Aniso Lower	Iso Higher	Iso Lower	
Refractive Parameters					
Spherical equivalent, D	−6.75 [−8.00–−5.75][a]	−4.12 [−5.19–−2.75][b]	−7.00 [−8.06–−4.88][a]	−6.62 [−7.62–−4.62][a]	*** <.001
Sphere, D	−6.50 [−7.62–−5.25][a]	−3.50 [−4.75–−2.00][b]	−6.00 [−7.50–−4.38][a]	−5.75 [−7.00–−4.25][a]	*** <.001
Cylinder, D	−1.00 [−1.62–−0.50]	−1.00 [−2.25–−0.50]	−1.25 [−1.75–−0.38]	−1.25 [−1.75–−0.38]	0.591
Keratometry					
Steep keratometry, D	43.95 [42.86–45.52]	44.23 [42.91–45.77]	43.89 [43.08–45.15]	43.89 [43.05–45.09]	0.81
Flat keratometry, D	42.61 [41.31–43.27]	42.45 [41.28–43.24]	42.40 [41.51–43.08]	42.40 [41.62–43.16]	0.984
Corneal Regularity Indices					
Surface regularity index	0.51 [0.34–0.68]	0.58 [0.43–0.80]	0.57 [0.39–0.71]	0.51 [0.32–0.69]	0.1
Surface asymmetry index	0.36 [0.32–0.42]	0.37 [0.32–0.41]	0.35 [0.32–0.42]	0.37 [0.30–0.41]	0.996
Asphericity (Q value)	−0.22 [−0.34–−0.08]	−0.24 [−0.34–−0.05]	−0.24 [−0.31–−0.08]	−0.21 [−0.37–−0.08]	0.95
Surface asymmetry (SA)	0.23 [0.18–0.28]	0.23 [0.16–0.28]	0.23 [0.19–0.29]	0.23 [0.18–0.29]	0.692
Shape deformation parameter	1.26 [1.06–1.45]	1.36 [1.13–1.56]	1.22 [1.05–1.46]	1.19 [1.04–1.44]	0.209
Kappa Angle					
Pupil kappa angle, °	0.18 [0.09–0.27]	0.20 [0.10–0.27]	0.20 [0.11–0.29]	0.19 [0.11–0.26]	0.812
Mesopic kappa angle, °	0.19 [0.11–0.26]	0.21 [0.12–0.30]	0.16 [0.11–0.26]	0.16 [0.10–0.26]	0.322
Higher-Order Aberrations (μm)					
Ocular spherical aberration	0.10 [0.06–0.17]	0.11 [0.06–0.18]	0.09 [0.05–0.15]	0.10 [0.05–0.15]	0.431
Ocular coma	0.19 [0.11–0.28]	0.19 [0.13–0.25]	0.16 [0.10–0.25]	0.17 [0.10–0.25]	0.477
Ocular trefoil	0.20 [0.12–0.30]	0.23 [0.16–0.31]	0.22 [0.14–0.31]	0.20 [0.13–0.26]	0.365
Total ocular HOA	0.37 [0.27–0.49]	0.39 [0.32–0.45]	0.33 [0.29–0.44]	0.33 [0.27–0.42]	0.104
Corneal spherical aberration	0.24 [0.18–0.28]	0.23 [0.16–0.28]	0.23 [0.19–0.29]	0.24 [0.18–0.29]	0.696

Characteristic	Anisometropia (n = 71)		Isometropia (n = 71)		P Value
Corneal coma	0.24 [0.15–0.29]	0.25 [0.17–0.28]	0.22 [0.14–0.32]	0.21 [0.15–0.31]	0.889
Corneal trefoil	0.19 [0.12–0.26][a]	0.18 [0.12–0.26][a]	0.14 [0.10–0.21][a]	0.14 [0.10–0.19][a]	** .004
Corneal HOA	0.42 [0.37–0.49]	0.41 [0.38–0.50]	0.41 [0.34–0.49]	0.39 [0.34–0.49]	0.361
Internal spherical aberration	0.15 [0.10–0.21]	0.17 [0.10–0.25]	0.17 [0.10–0.26]	0.15 [0.11–0.21]	0.684
Internal coma	0.21 [0.16–0.28]	0.19 [0.12–0.27]	0.20 [0.15–0.28]	0.22 [0.16–0.28]	0.209
Internal trefoil	0.18 [0.10–0.24]	0.19 [0.14–0.25]	0.17 [0.10–0.23]	0.15 [0.11–0.21]	0.191
Internal HOA	0.37 [0.30–0.49]	0.40 [0.33–0.45]	0.37 [0.31–0.44]	0.37 [0.30–0.44]	0.711

IQR = 25th–75th percentile; HOA = higher-order aberrations; Aniso Higher = anisometropia higher-refraction eye; Aniso Lower = anisometropia lower-refraction eye.

Part A: Mann–Whitney U test (continuous variables); chi-square test (sex). Part B: Kruskal–Wallis test across 4 groups; post-hoc pairwise Mann–Whitney U with Bonferroni correction.

Shared superscript letters indicate no statistically significant pairwise difference (P > .05 after correction).

** P < .01; *** P < .001.

Absolute Higher-Order Aberrations and Association with Anisometropia

Initial evaluation of absolute higher-order aberration (HOA) profiles revealed no significant differences across the four subgroups (all P > .05). Although absolute corneal trefoil exhibited a significant main effect (P = .004), subsequent Bonferroni-corrected pairwise comparisons revealed no significant differences.

To further investigate the independent effect of anisometropia on absolute HOAs, generalized estimating equation (GEE) models were utilized, adjusting for within-subject interocular correlation, spherical equivalent, age, and sex (Table 2). At the ocular, corneal, and internal levels, corneal trefoil emerged as the sole parameter demonstrating a significant independent elevation in the anisometropia group (β = 0.0510; 95% CI: 0.0186–0.0833; Wald χ^2 = 9.551; P = .002). Consequently, the anisometropic condition was independently associated with greater corneal trefoil, regardless of the baseline refractive error. All other absolute HOA parameters failed to reach statistical significance between the groups (all P > .05).

Table 2. Association Between Higher-Order Aberrations and Anisometropia: Generalized Estimating Equation Analysis

HOA Parameter	β Coefficient	Standard Error	95% CI		Wald χ2	P Value
			Lower	Upper		
Ocular aberrations						
Spherical aberration	0.0154	0.0129	−0.0098	0.0406	1.432	0.231
Coma	0.0081	0.0171	−0.0254	0.0416	0.226	0.634
Trefoil	0.0226	0.018	−0.0127	0.0578	1.577	0.209
Total HOA	0.0303	0.0207	−0.0103	0.0708	2.137	0.144
Corneal aberrations						
Spherical aberration	−0.0154	0.0127	−0.0402	0.0095	1.471	0.225
Coma	−0.0043	0.0185	−0.0406	0.032	0.055	0.815
Trefoil **	0.051	0.0165	0.0186	0.0833	9.551	0.002
Total HOA	0.0188	0.0184	−0.0172	0.0548	1.047	0.306
Internal aberrations						
Spherical aberration	−0.0074	0.018	−0.0427	0.0279	0.169	0.681
Coma	−0.0039	0.0126	−0.0285	0.0207	0.096	0.757
Trefoil	0.0256	0.0156	−0.0050	0.0562	2.693	0.101
Total HOA	0.017	0.0175	−0.0172	0.0513	0.954	0.329

GEE = generalized estimating equations; HOA = higher-order aberrations; CI = confidence interval.

Each row represents a separate GEE model with exchangeable working correlation structure, adjusting for the paired eye structure within participants.

The dependent variable is the absolute HOA value (μm). The independent variable of interest is group (Anisometropia vs. Isometropia), adjusting for covariates including spherical equivalent, age, and sex.

β represents the adjusted mean difference in HOA (μm) between the anisometropia and isometropia groups (reference). A positive β indicates a higher aberration magnitude in the anisometropia group.

P < .01.

Interocular HOA Asymmetry: Within-Group and Between-Group Comparisons

Within-Group Profiles

While group-level comparisons of absolute values yielded no significant differences, population averages can inherently exert a masking effect on individual-level variations. To bypass this limitation, we further expanded our analysis to evaluate interocular asymmetry at the individual level.

Paired analyses within the anisometropic group showed no significant interocular differences across most HOA parameters. Internal coma was the sole exception, presenting significantly higher values in the Aniso Higher eyes (median: 0.213 vs. 0.194 μm; P = .031). Conversely, the isometropic group demonstrated bilateral symmetry across all evaluated parameters (all P > .05) (Table 3).

Magnitude of Interocular Differences

Evaluation of the absolute interocular difference (denoted as |Δ| Parameter) revealed that the anisometropia group exhibited significantly greater asymmetry across multiple optical levels (ocular, corneal, and internal) (Table 3). Specifically, interocular differences in total HOAs were larger in anisometropic participants at the ocular (median |Δ|: 0.108 vs. 0.077 μm; P = .020), corneal (0.071 vs. 0.052 μm; P = .009), and internal (0.096 vs. 0.073 μm; P = .033) levels, yielding moderate effect sizes (Cohen's d: 0.385–0.544). Notably among individual aberrations, corneal coma asymmetry was profoundly more pronounced in the anisometropia cohort (0.082 vs. 0.054 μm; P = .004). As depicted in Figure 1, the anisometropic group exhibited broader data dispersion and higher medians. Conversely, no significant differences were detected between the two groups for the remaining aberrations, including spherical aberration and trefoil at all levels, as well as ocular and internal coma (all P > .05).

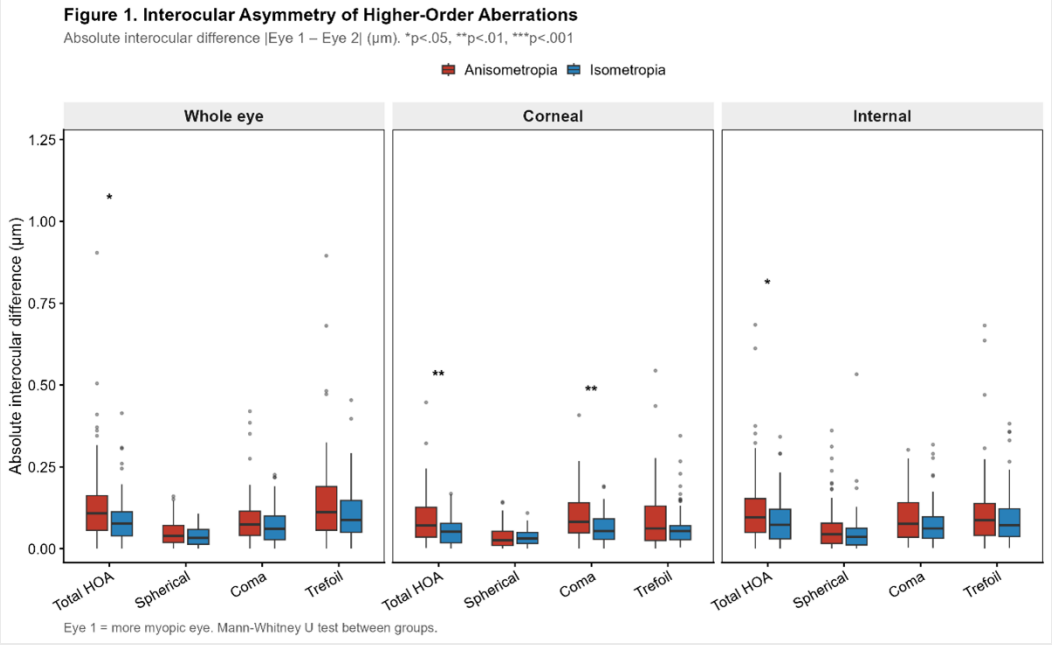

Figure 1. Interocular asymmetry of higher-order aberrations (HOAs) in the anisometropia and isometropia groups. Box plots show the absolute interocular difference (|Eye 1 − Eye 2|, in μm) for total HOA, spherical aberration, coma, and trefoil, partitioned into whole-eye (left), corneal (middle), and internal (right) components. Eye 1 denotes the more myopic eye. Boxes represent the interquartile range (IQR, 25th–75th percentiles) with the horizontal line indicating the median; whiskers extend to 1.5 × IQR, and points beyond the whiskers represent outliers. Red boxes, anisometropia; blue boxes, isometropia. Between-group comparisons were performed using the Mann–Whitney U test (*p < .05, **p < .01, ***p < .001).

Table 3. Interocular Asymmetry in Higher-Order Aberrations: Within-Group and Between-Group Comparisons

HOA Parameter	Anisometropia (n = 71)		Isometropia (n = 71)		|Δ| Anisometropia Median [IQR]	|Δ| Isometropia Median [IQR]	P (Aniso)	P (Iso)	U Statistic	P Value	Cohen's d	Sig.
	Higher Eye	Lower Eye Median [IQR]	Eye 1 Median [IQR]	Eye 2 Median [IQR]								
Ocular aberrations												
Spherical aberration	0.104 [0.058–0.166]	0.112 [0.056–0.181]	0.086 [0.054–0.145]	0.098 [0.053–0.148]	0.039 [0.019–0.071]	0.033 [0.013–0.059]	0.582	0.232	2899.5	0.122	0.366	
Coma	0.189 [0.112–0.275]	0.194 [0.134–0.249]	0.161 [0.104–0.247]	0.173 [0.096–0.249]	0.074 [0.040–0.115]	0.061 [0.028–0.100]	0.643	0.956	2814	0.232	0.267	
Trefoil	0.198 [0.123–0.299]	0.226 [0.158–0.309]	0.221 [0.137–0.311]	0.195 [0.127–0.261]	0.112 [0.056–0.190]	0.088 [0.050–0.148]	0.409	0.309	2923	0.101	0.336	
Total HOA	0.370 [0.273–0.487]	0.394 [0.316–0.453]	0.331 [0.289–0.436]	0.334 [0.272–0.422]	0.108 [0.056–0.162]	0.077 [0.039–0.113]	0.665	0.686	3093	0.02	0.418	*
Corneal aberrations												
Spherical aberration	0.236 [0.180–0.279]	0.232 [0.162–0.279]	0.235 [0.190–0.293]	0.237 [0.183–0.291]	0.026 [0.010–0.053]	0.031 [0.016–0.050]	0.228	0.879	2334	0.448	0.049	
Coma	0.242 [0.152–0.291]	0.247 [0.172–0.282]	0.223 [0.136–0.319]	0.209 [0.148–0.307]	0.082 [0.048–0.141]	0.054 [0.028–0.091]	0.349	0.873	3234.5	0.004	0.557	**
Trefoil	0.193 [0.121–0.263]	0.176 [0.121–0.262]	0.141 [0.102–0.207]	0.140 [0.098–0.191]	0.062 [0.025–0.130]	0.054 [0.027–0.071]	0.352	0.241	2773	0.304	0.266	
Total HOA	0.422 [0.366–0.493]	0.412 [0.376–0.495]	0.412 [0.342–0.485]	0.392 [0.343–0.494]	0.071 [0.036–0.126]	0.052 [0.018–0.078]	0.961	0.331	3157.5	0.009	0.544	**
Internal aberrations												
Spherical aberration	0.150 [0.101–0.210]	0.167 [0.097–0.249]	0.171 [0.104–0.257]	0.148 [0.108–0.213]	0.044 [0.016–0.078]	0.036 [0.012–0.062]	0.333	0.106	2895.5	0.126	0.247	
Coma	0.213 [0.161–0.282]	0.194 [0.120–0.267]	0.202 [0.152–0.279]	0.219 [0.158–0.282]	0.076 [0.035–0.141]	0.062 [0.032–0.098]	.031 *	0.594	2874	0.15	0.241	
Trefoil	0.176 [0.102–0.238]	0.188 [0.136–0.250]	0.168 [0.096–0.228]	0.152 [0.107–0.214]	0.087 [0.040–0.139]	0.072 [0.037–0.122]	0.378	0.669	2703.5	0.457	0.168	
Total HOA	0.371 [0.302–0.491]	0.396 [0.328–0.452]	0.373 [0.309–0.445]	0.373 [0.300–0.442]	0.096 [0.049–0.153]	0.073 [0.030–0.120]	0.905	0.902	3044	0.033	0.385	*

|Δ| = absolute interocular difference (μm); HOA = higher-order aberrations; IQR = interquartile range.

Wilcoxon signed-rank test comparing higher vs lower refraction eye (anisometropia group) or Eye 1 vs Eye 2 (isometropia group).

* P < .05.

|Δ| = absolute interocular difference (μm); HOA = higher-order aberrations; IQR = interquartile range.

Mann–Whitney U test comparing absolute interocular HOA difference between anisometropia and isometropia groups. Cohen's d calculated on absolute difference values as effect size estimate.

cohen's d was computed from raw values as an approximate effect size estimate for descriptive purposes, alongside the non-parametric test results.

* P < .05; ** P < .01.

Correlates of Interocular HOA Asymmetry and Multivariable Regression

Spearman Rank Correlations

HOA asymmetry was not significantly correlated with interocular spherical equivalent differences or the magnitude of myopia in the more myopic eye (all P > .05) (Table 4). Among corneal indices, the absolute interocular difference in the SAI (|ΔSAI|) showed the strongest associations. (Table 4 and Figure 2) Positive correlations were observed between |ΔSAI| and asymmetry in corneal coma (rs = 0.402, P < .001), total corneal HOAs (rs = 0.407, P < .001), and internal HOAs (rs = 0.277, P = .019). Significance was maintained for both corneal HOA associations after Benjamini–Hochberg false discovery rate correction, whereas the association with internal HOAs did not survive the correction. Furthermore, |ΔQ-value| was positively correlated with asymmetry in total ocular (rs = 0.244, P = .041) and total corneal (rs = 0.249, P = .036) HOAs. Positive correlations were also observed between |ΔSA| and total corneal HOA asymmetry (rs = 0.257, P = .031). Conversely, |ΔSRI| was inversely correlated with internal HOA asymmetry (rs = −0.257, P = .030).

Table 4. Correlates of Interocular HOA Asymmetry and Multivariable Regression Models in the Anisometropia Group (n = 71)

Predictor Variable	Total Ocular HOA		Corneal Coma		Corneal HOA		Internal HOA	
	rs	P	rs	P	rs	P	rs	P
Refractive and demographic								
Interocular SE difference, D	−0.151	0.209	0.156	0.194	0.106	0.377	−0.141	0.239
SE of more myopic eye, D	0.155	0.198	0.025	0.836	0.019	0.878	−0.151	0.209
Age, years	0.015	0.902	0.224	.060†	−0.087	0.472	0.034	0.781
Keratometry								
|Δ Steep keratometry|, D	−0.040	0.742	0.049	0.684	0.179	0.135	−0.083	0.49
|Δ Flat keratometry|, D	−0.199	.097†	−0.082	0.496	−0.125	0.301	−0.104	0.389
Corneal regularity indices								
|Δ Surface regularity index|	−0.141	0.241	0.093	0.441	0.003	0.978	−0.257	.030*
|Δ Surface asymmetry index|	0.146	0.223	0.402	<.001***†	0.407	<.001***†	0.277	.019*
|Δ Asphericity (Q value)|	0.244	.041*	0.228	.055†	0.249	.036*	0.111	0.357
|Δ Spherical aberration (SA)|	−0.012	0.924	0.041	0.734	0.257	.031*	0.038	0.752
|Δ Shape deformation parameter|	−0.014	0.91	0.098	0.414	0.087	0.469	−0.048	0.691

HOA = higher-order aberrations

SE = spherical equivalent;

|Δ| = absolute interocular difference.

† P < .10 (trend); * P < .05

*** P < .001. Superscript † after significance asterisks

(†***) indicates association also significant after Benjamini–Hochberg FDR correction (PFDR < .05).

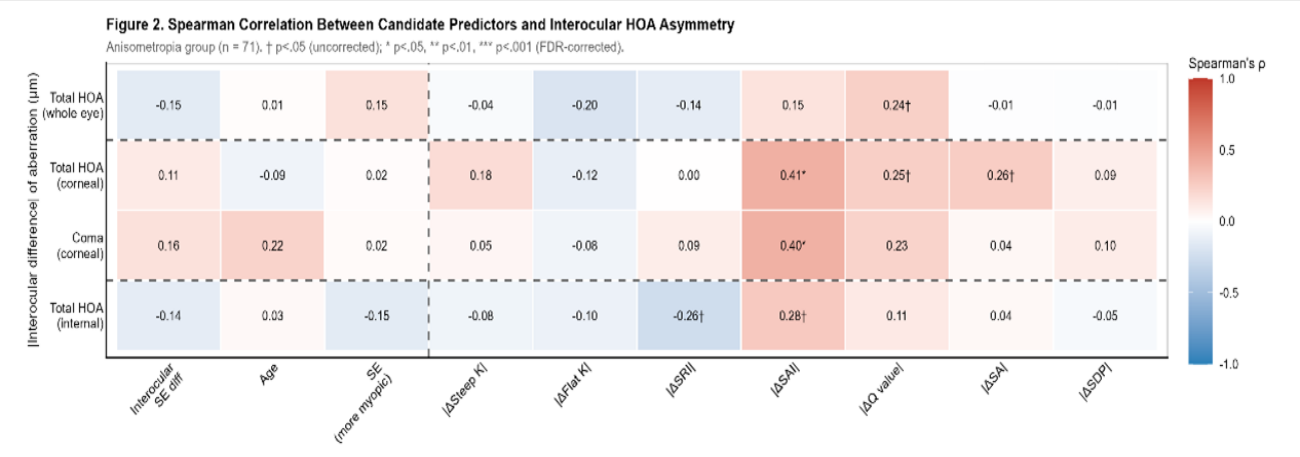

Figure 2. Spearman correlations between candidate predictors and interocular asymmetry of higher-order aberrations (HOAs) in the anisometropia group (n = 71). The heatmap displays Spearman's rank correlation coefficients (ϱ) between each predictor (columns) and the absolute interocular difference in HOA magnitude (rows; |Eye 1 − Eye 2|, μm), where Eye 1 denotes the more myopic eye. Cell color encodes the strength and direction of correlation (red, positive; blue, negative), and the numeric value in each cell is the corresponding ϱ. Rows comprise total HOA of the whole eye, total corneal HOA, corneal coma, and total internal HOA. Columns are grouped by the vertical dashed line into demographic/refractive factors (interocular spherical-equivalent difference, age, and spherical equivalent of the more myopic eye) and interocular differences in corneal/optical parameters (|ΔSteep K|, |ΔFlat K|, |ΔSRI|, |ΔSAI|, |ΔQ value|, |ΔSA|, and |ΔSDP|). Statistical significance: † p < .05 (uncorrected); * p < .05, ** p < .01, *** p < .001 (FDR-corrected for multiple comparisons).

Multivariable Linear Regression

Variables demonstrating P < .10 in the univariable Spearman analyses were incorporated into multivariable linear regression models (Table 5). |ΔSAI| emerged as a significant independent predictor of asymmetry in corneal coma (β = 0.589; 95% CI: 0.318–0.860; P < .001), total corneal HOAs (β = 0.423; 95% CI: 0.164–0.682; P = .002), and internal HOAs (β = 0.682; 95% CI: 0.197–1.166; P = .007). Similarly, |ΔQ-value| independently predicted total corneal HOA asymmetry (β = 0.105; 95% CI: 0.058–0.152; P < .001). No independent significance was observed for the remaining parameters, including age, magnitude of refractive error, and interocular differences in keratometry.

DISCUSSION

This cross-sectional study systematically characterized higher-order aberration (HOA) profiles and their interocular asymmetry in 71 young adults with myopic anisometropia and 71 isometropic controls, yielding three principal findings. First, the presence of anisometropia was independently associated with an elevated magnitude of absolute corneal trefoil in GEE models, serving as the sole affected single-eye parameter. Second, despite comparable absolute HOA values at the single-eye level, anisometropic participants exhibited significantly greater interocular asymmetry across total, corneal, and internal HOAs, particularly in corneal coma. Third, the absolute interocular difference in the surface asymmetry index (|ΔSAI|) emerged as the dominant independent predictor of interocular HOA asymmetry, demonstrating a stronger association than absolute refractive error or the interocular refractive difference itself. These findings suggest that the optical consequences of anisometropia are better characterized as binocular wavefront imbalance than as unilateral aberrational excess, with corneal surface irregular asymmetry as its principal structural correlate.

Among all HOA parameters examined, only corneal trefoil showed a statistically significant independent elevation in the anisometropia cohort. This selectivity is notable given that coma and spherical aberration, parameters more commonly implicated in progressive myopia, failed to reach significance.

Trefoil (Z_3^{-3} and Z_3^{+3}) reflects irregular meridional corneal asymmetry not captured by conventional keratometry or cylinder power. Its association with anisometropia degree suggests that this asymmetrical refractive condition is accompanied by subtle, non-uniform deformation in the cornea of the more ametropic eye. Prior animal models and clinical investigations indicate that interocular differences in axial elongation and altered biomechanical loading are frequently associated with asymmetric stromal remodeling, particularly at the paracentral and peripheral cornea where trefoil components are highly sensitive[22-24].

Importantly, this association was confined to the corneal component; internal and total ocular trefoil were not significantly associated. This specificity points toward anterior corneal surface remodeling rather than a global optical pathway effect. The discordance between the significant main effect in four-group comparisons and the absence of surviving pairwise differences after Bonferroni correction is consistent with the GEE result: corneal trefoil serves as a sensitive indicator of the overall anisometropic condition rather than distinguishing discrete subgroups. Clinically, this positions corneal trefoil as a continuously scaled indicator of anisometropia-associated corneal change, which may be detectable even when conventional topography parameters appear grossly stable[23].

Table 5. Correlates of Interocular HOA Asymmetry and Multivariable Regression Models in the Anisometropia Group (n = 71)

Predictor	Total Ocular HOA			Corneal Coma			Corneal HOA			Internal HOA		
	β	95% CI	P	β	95% CI	P	β	95% CI	P	β	95% CI	P
|Δ Flat keratometry|, D	−0.074	[−0.189, 0.041]	0.21	—	—	—	—	—	—	—	—	—
|Δ Surface regularity index|	—	—	—	—	—	—	—	—	—	−0.105	[−0.293, 0.083]	0.278
|Δ Surface asymmetry index|	—	—	—	0.589	[0.318, 0.860]	<.001***	0.423	[0.164, 0.682]	.002**	0.682	[0.197, 1.166]	.007**
|Δ Asphericity (Q value)|	0.061	[−0.036, 0.159]	0.224	0.011	[−0.035, 0.057]	0.645	0.105	[0.058, 0.152]	<.001***	—	—	—
|Δ Spherical aberration (SA)|	—	—	—	—	—	—	0.429	[−0.022, 0.881]	.067†	—	—	—
Age, years	—	—	—	0.002	[−0.001, 0.005]	0.126	—	—	—	—	—	—

β = unstandardized regression coefficient (μm per unit change in predictor). 95% CI = 95% confidence interval.

— = predictor not included in that model. Models were constructed from variables reaching P < .10 in Part A Spearman analysis.

† P < .10 (trend); ** P < .01; *** P < .001.

A defining feature of the present data is the dissociation between single-eye HOA magnitude and interocular HOA asymmetry. Absolute HOA values across all 12 parameters did not differ significantly across the four eye subgroups. Yet interocular HOA differences were significantly larger in anisometropic participants at every optical level: ocular total HOA, corneal total HOA, internal total HOA, and corneal coma specifically, demonstrating moderate effect sizes.

This pattern indicates that anisometropia's optical profile in myopic anisometropia is characterized by a systemic misalignment of wavefront profiles between the two eyes rather than a degradation in the optical quality of either eye individually. The visual cortex is highly sensitive to interocular differences in spatial frequency content and aberration structure[25,26]. Moderate binocular disparities in wavefront profile can disrupt fusion, impair stereoacuity, and promote amblyopia through competitive suppression[27]. In young adults with anisometropia, the primary optical threat to binocular vision may therefore reside not in the absolute quality of either eye, but in their optical mismatch.

Within the anisometropic group, paired analysis identified internal coma as the sole parameter significantly elevated in the more myopic eye. Internal aberrations are conventionally attributed to the crystalline lens and its alignment relative to the optical axis[28]. Elevated internal coma in the higher-myopia eye may reflect lens tilt or decentration or asymmetric compensatory lenticular remodeling accompanying greater axial growth[28,29]. Prior work has shown that the crystalline lens partially compensates for corneal aberrations in emmetropic eyes[30], whether this compensatory coupling is disrupted asymmetrically in anisometropia warrants prospective longitudinal verification.

Spearman rank correlations identified |ΔSAI| as the most consistently associated variable with interocular HOA asymmetry, with significant positive correlations for corneal coma, total corneal HOA, and internal HOA. The corneal associations survived Benjamini–Hochberg FDR correction. In multivariable regression, |ΔSAI| remained a strong independent predictor of asymmetry in all three components.

The SAI quantifies the non-rotationally symmetric component of corneal power, reflecting irregular astigmatism that deviates from a smooth conic surface[31]. Unlike mean keratometry or Q-value, which characterize central curvature and prolate-oblate shape respectively, the SAI is sensitive to localized irregularities distributed across the analyzed ring diameter. The primacy of |ΔSAI| over the interocular SE difference implies that refractive disparity is a poor surrogate for binocular optical quality mismatch.

The independent association of |ΔSAI| with internal HOA asymmetry further suggests cross-component coupling: corneal surface asymmetry differences are propagated through, and possibly amplified by, the internal optics. This likely reflects incomplete lenticular compensation for corneal aberrations in an asymmetric optical system. The independent prediction of total corneal HOA asymmetry by |ΔQ-value| is consistent with the established asphericity-aberration relationship governing peripheral corneal HOA generation[32,33].

The absence of any significant correlation between anisometropia degree and interocular HOA asymmetry is noteworthy. Neither the interocular spherical equivalent difference nor the absolute refraction of the more myopic eye predicted HOA asymmetry at any optical level. This decoupling suggests that differential axial elongation does not translate uniformly into corneal irregularity or wavefront imbalance. The magnitude of the refractive disparity reflects axial length asymmetry but not corneal topographic asymmetry, which appears governed by distinct biomechanical or developmental mechanisms.

Clinically, refractive difference alone is insufficient for optical quality assessment in anisometropia. Corneal topographic indices, particularly the SAI, carry more information about binocular optical compatibility than the spherical equivalent difference. In refractive surgery candidates with anisometropia, high |ΔSAI| may identify patients with disproportionate binocular optical asymmetry that warrants targeted management beyond standard refractive correction.

CONCLUSIONS

In young adults with myopic anisometropia, the optical consequences are best characterized as binocular wavefront imbalance rather than unilateral aberrational excess. Corneal trefoil uniquely scales with anisometropia severity, implicating progressive asymmetric corneal deformation as a feature of increasing interocular refractive disparity. Interocular HOA asymmetry is significantly amplified across ocular, corneal, and internal levels, with moderate effect sizes. This imbalance is driven not by the degree of refractive difference, but by asymmetry in corneal surface regularity as quantified by the SAI. Comprehensive optical assessment of anisometropic patients should therefore extend beyond spherical equivalent differences to include binocular wavefront compatibility and corneal topographic symmetry.

ACKNOWLEDGEMENT

None

FUNDING

National Key Research and Development Program of China (Grant No. 2022YFC2404505). The funding organization had no role in the design or conduct of this research.

CONFLICT OF INTEREST

The author declares no potential conflicts of interest with respect to the research, authorship, and/or publication of this article.

REFERENCES

1. Evans BJ, Shah R, Vlasak N. The changing natural history of anisometropia: a scoping review. *Ophthalmic Physiol Opt.* 2026;46(1):13-28.
2. Kinori M, Nitzan I, Szyper NS, Achiron A, Spierer O. Correlation of refractive error with anisometropia development in early childhood. *Am J Ophthalmol.* 2024;264:145-153.
3. Xu Z, Wu Z, Wen Y, et al. Prevalence of anisometropia and associated factors in Shandong school-aged children. *Front Public Health.* 2022;10:1072574.
4. Ostadimoghaddam H, Fotouhi A, Hashemi H, et al. The prevalence of anisometropia in a population-based study. *Strabismus.* 2012;20(4):152-157.
5. Hashemi H, Khabazkhoob M, Yekta A, Mohammad K, Fotouhi A. Prevalence and risk factors for anisometropia in the Tehran Eye Study, Iran. *Ophthalmic Epidemiol.* 2011;18(3):122-128.
6. Abdelzaher HA, Sidky MK, Awadein A, Hosny M. Aniseikonia and visual functions with optical correction and after refractive surgery in axial anisometropia. *Int Ophthalmol.* 2022;42(6):1669-1677.
7. South J, Gao T, Collins A, et al. Aniseikonia and anisometropia: implications for suppression and amblyopia. *Clin Exp Optom.* 2019;102(6):556-565.
8. Bharadwaj SR, Candy TR. The effect of lens-induced anisometropia on accommodation and vergence during human visual development. *Invest Ophthalmol Vis Sci.* 2011;52(6):3595-3603.
9. Cakir GB, Murray J, Dulaney C, Ghasia F. Multifaceted interactions of stereoacuity, interocular suppression, and fixation eye movement abnormalities in amblyopia and strabismus. *Invest Ophthalmol Vis Sci.* 2024;65(3):19.
10. Mestre C, Candy TR. The impact of simulated anisometropia and bilateral defocus on reflex vergence responses of children and adults. *Invest Ophthalmol Vis Sci.* 2026;67(2):43.
11. Wang D, Chang Y, Nan W, Zhang Y. Comparative analysis of corneal parameters in simple myopic anisometropia using Scheimpflug technology. *Front Bioeng Biotechnol.* 2024;12:1366408.
12. Zhang Y, Li J, Wei S, et al. Characteristics of anterior and posterior ocular biometric parameters in nonamblyopic myopic anisometropia. *Eye Contact Lens.* 2025;51(11):491-497.
13. Hoshing A, Samant M, Bhosale S, Naik AM. Comparison of higher order aberrations in amblyopic and non-amblyopic eyes in pediatric patients with anisometropic amblyopia. *Indian J Ophthalmol.* 2019;67(7):1025-1029.
14. Seo JY, Kwon NE, Jun JH, Bang SP. Distribution and demographic correlates of ocular wavefront aberrations in a Korean population. *J Clin Med.* 2025;14(19):6981.
15. Artal P, Guirao A, Berrio E, Williams DR. Compensation of corneal aberrations by the internal optics in the human eye. *J Vis.* 2001;1(1):1-8.
16. Zhang H, Zhao J, Chen H, et al. Large-dynamic-range ocular aberration measurement based on deep learning with a Shack-Hartmann wavefront sensor. *Sensors (Basel).* 2024;24(9):2728.
17. Vacalebre M, Frison R, Corsaro C, et al. Advanced optical wavefront technologies to improve patient quality of vision and meet clinical requests. *Polymers (Basel).* 2022;14(23):5321.

18. Govind I, Antony C, Jacob SC, Kalikivayi V. Ocular higher order aberrations: a comparison between myopes and emmetropes. *Oman J Ophthalmol.* 2026;19(1):59-64.
19. Kasahara K, Maeda N, Fujikado T, et al. Characteristics of higher-order aberrations and anterior segment tomography in patients with pathologic myopia. *Int Ophthalmol.* 2017;37(6):1279-1288.
20. Hashemi H, Mesbahi S, Jamali A, et al. The association between ocular biometric components and corneal aberrations. *Clin Exp Optom.* 2024;107(6):609-615.
21. McGinnigle S, Naroo SA, Eperjesi F. Evaluation of the auto-refraction function of the Nidek OPD-Scan III. *Clin Exp Optom.* 2014;97(2):160-163.
22. Chen L, Huang Y, Zhang X, et al. Corneal biomechanical properties demonstrate anisotropy and correlate with axial length in myopic eyes. *Invest Ophthalmol Vis Sci.* 2023;64(10):27.
23. Vincent SJ, Collins MJ, Read SA, Carney LG. Monocular amblyopia and higher order aberrations. *Vision Res.* 2012;66:39-48.
24. Alzaben Z, Gammoh Y, Freixas M, Zaben A, Zapata MA, Koff DN. Inter-ocular asymmetry in anterior corneal aberrations using Placido disk-based topography. *Clin Ophthalmol.* 2020;14:1451-1457.
25. Devi P, Kumar P, Marella BL, Bharadwaj SR. Impact of degraded optics on monocular and binocular vision: lessons from recent advances in highly-aberrated eyes. *Semin Ophthalmol.* 2022;37(7-8):869-886.
26. Neroev V, Tarutta E, Khodzhabekyan N, Khandzhyan A, Arutyunyan S. Anatomical and optical parameters and aberrations of the optical system of the eye in anisometropic myopia. *Russian Ophthalmol J.* 2023;16(2):47-53.
27. Martino F, Castro-Torres JJ, Casares-López M, et al. Effect of interocular differences on binocular visual performance after inducing forward scattering. *Ophthalmic Physiol Opt.* 2022;42(4):730-743.
28. Zhang J, Jin G, Jin L, et al. Profiles of intraocular higher-order aberrations in healthy phakic eyes: prospective cross-sectional study. *Ann Transl Med.* 2020;8(14):850.
29. Muralidharan G, Martínez-Enríquez E, Birkenfeld J, Velasco-Ocana M, Pérez-Merino P, Marcos S. Morphological changes of human crystalline lens in myopia. *Biomed Opt Express.* 2019;10(12):6084-6095.
30. Berrio E, Tabernero J, Artal P. Optical aberrations and alignment of the eye with age. *J Vis.* 2010;10(14):34.
31. Dingeldein SA, Klyce SD, Wilson SE. Quantitative descriptors of corneal shape derived from computer-assisted analysis of photokeratographs. *J Refract Surg.* 1989;5(6):372-378.
32. He JC. Theoretical model of the contributions of corneal asphericity and anterior chamber depth to peripheral wavefront aberrations. *Ophthalmic Physiol Opt.* 2014;34(3):321-330.
33. Wu CZ, Cui X, Li ZR, et al. Study on the corneal higher-order aberrations and correlation in patients with different degrees of myopia suitable for wavefront-guided FS-LASIK. *J Biosci Med.* 2020;8(1):13-22.